ISSN (Print) 1226-1750
ISSN (Online) 2233-6656
Journal of Magnetics 28(4), 403-408 (2023) https://doi.org/10.4283/JMAG.2023.28.4.403

A Feasibility Study of GPU-Accelerated Image Reconstruction with Distance-Driven Method in Digital Tomosynthesis Utilizing Rectilinear Geometry in the LINAC System

Byungdu Jo[1,2]*

[1]*Department of Radiological Science, Dongseo University, Busan 47011, Republic of Korea*
[2]*Center for Radiological Environment & Health Science, Dongseo University, Busan 47011, Republic of Korea*

(Received 6 October 2023, Received in final form 5 December 2023, Accepted 5 December 2023)

External Beam Radiation Therapy (EBRT) remains a mainstay in cancer treatment. Accurate patient positioning and beam alignment are essential for optimal therapeutic outcomes. However, ensuring the correct patient positioning can be challenging during radiation treatment sessions. This study focuses on the development and validation of a kV X-ray based rectilinear geometry digital tomosynthesis (DTS) system tailored for the LINAC system within EBRT. Additionally, we emphasize the enhancement of the DTS image reconstruction speed via GPU-based CUDA programming and its potential implications for real-time patient alignment and monitoring. Through modeling the rectilinear geometry DTS system, we obtained the projection images crucial for reconstruction. The acquired images were reconstructed using various algorithms. The impact of GPU-based CUDA programming on speeding up the reconstruction process was also examined. As a result, acceleration factors of up to 30 % times were achieved compared to a single thread CPU implementation. This study underscores the potential of GPU-Accelerated image reconstruction using the distance-driven method in DTS with rectilinear geometry for the LINAC System. By applying this technique to the EBRT system, it is feasible to position patients using reconstructed tomographic images in real-time using kV tomography images, even in the absence of an On-board imaging (OBI).

Keywords : digital tomosynthesis, GPU-acceleration, image reconstruction, electro-magnetic radiation, rectilinear geometry, linear accelerator magnetrons

1. Introduction

External beam radiation therapy (EBRT) is the predominant treatment method for the majority of cancer patients. While accurate patient positioning and beam alignment are essential for optimal treatment outcomes, variations and errors in patient setup can still arise during the radiation treatment process. To mitigate these challenges and ensure precise alignment, Image-guided Radiotherapy is employed, adjusting for any shifts in both patient position and target location before every treatment session [1, 2]. Current strategies for patient positioning in the LINAC system employ a wide spectrum of techniques. These include ultrasound [3], Magnetic Resonance Imaging (MRI) [4, 5], electronic portal imaging device (EPID) [6], Cone-Beam Computed Tomography (CBCT)-guided methods utilizing both kilovolt (kV) and megavolt (MV) settings [7] and state-of-the-art 4D techniques like gating, tracking, and breath holding [8], among others. Within this diverse spectrum of techniques, conventional practices demonstrate a distinct preference for CBCT in radiotherapy positioning, owing to the heightened contrast afforded by kV imaging. Especially, On-board imaging (OBI) systems, which capture CBCT images, have emerged as a premier choice, offering the advantage of obtaining planar images and the capability of real-time image reconstruction. However, the integration of On-board imaging (OBI) systems faces obstruction due to their substantial cost, causing many facilities to lack the capacity to harness CBCT imaging.

Recently, there has been a growing interest in utilizing kV X-ray sources for the acquisition of tomographic images via a method termed digital tomosynthesis (DTS) [9-11]. Siemens Medical Solutions' Oncology Care Systems Group was the pioneer in introducing the design

*Corresponding author: Tel: +82-51-320-4274
e-mail: byungdujo@gdsu.dongseo.ac.kr

of a multisource DTS system for patient setup and motion management in internal beam radiation therapy, effectively integrating DTS technology with the EPID within a LINAC system [12]. This integration yields enhanced image quality, reduced patient exposure to radiation, and potential real-time feedback, making it a promising avenue for research and development. This paradigm shift has catalyzed further research into the configuration of multi-array X-ray sources specifically designed for LINAC systems.

Furthermore, a significant challenge in image-guided radiation therapy lies in the need for rapid reconstruction speeds for 3D or 4D images to enhance the efficacy of IGRT procedures [13]. Given the intensive computational demands of various reconstruction algorithms, there is a consensus that parallel processing is crucial to achieve practical processing durations [14]. Remarkably, such an approach reduced the computational time from several hours to a few minutes [15]. Consequently, the integration of GPU-focused strategies suggests potential for even more precise treatment outcomes.

In this study, the development of a graphics processing unit (GPU)-accelerated image reconstruction techniques with distance-driven method in rectilinear geometry DTS for LINAC system is described. The central objective of this study is to assess the effectiveness of incorporating GPU-centric Compute Unified Device Architecture (CUDA) programming to expedite the projection operators in DTS image reconstruction, ultimately aiming to improve real-time patient alignment and kinematic monitoring within the framework of rectilinear geometry DTS.

2. Materials and Methods

2.1. Rectilinear geometry DTS system configuration

The rectilinear geometry DTS system was designed using a Varian True Beam linear accelerator in conjunction with the Varian aS1200 EPID (Varian Medical Systems, Palo Alto, CA). Within this system, the X-ray tube is strategically positioned on the gantry of the LINAC directly below the multi-leaf collimator and is securely anchored by mounting brackets. This configuration permits direct acquisition of attenuated signals from the X-ray tube to the EPID, leading to image formation as depicted in Fig. 1(a). Throughout the study, an X-ray tube was employed, acquiring 52 projection images in a rectilinear geometry with intervals of 1 cm between them, as highlighted in Fig. 1(b). Significantly, this DTS system setup enables the acquisition of tomographic projections using a kV X-ray tube, without requiring LINAC gantry rotation. In terms of tomographic imaging, the aS1200 EPID typically features an active imaging area of 43 × 43 cm^2 and is equipped with a pixel array of 1280 × 1280, resulting in a pixel pitch of 0.336 mm.

For the purpose of computational efficiency, projection images were obtained at a resolution of 160 × 160, deviating from the conventional 1280 × 1280 resolution. Regarding the image acquisition specifications, both the kV source-to-object distance (SOD) and the object to

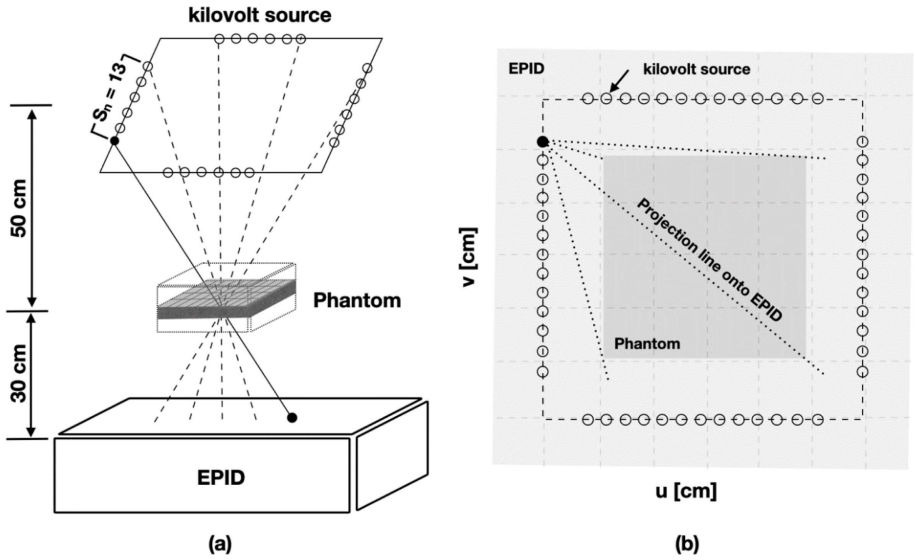

Fig. 1. A schematic illustrations of the rectilinear geometry DTS system. (a) X-ray tube positioning below the multi-leaf collimator, showing the direct acquisition pathway of attenuated signals to the EPID, (b) is top view of the acquisition trajectories in a rectilinear geometry.

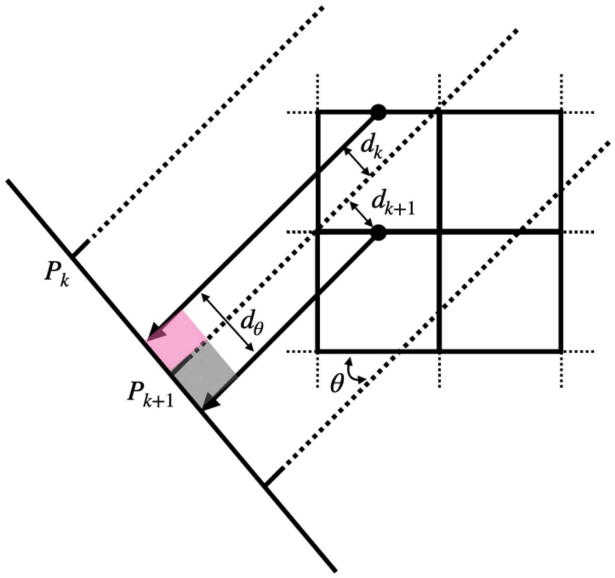

Fig. 2. (Color online) Representation of distance-driven projection. The two corresponding weighting coefficients are : d_k/d_θ, d_{k+1}/d_θ. The detector boundaries are denote by P_k, pixel boundaries by d_k.

detector distance (ODD) set at 50 cm and 30 cm, respectively.

2.2. Distance-driven projection

Tomosynthesis image reconstruction via distance-driven projection entails intricate calculations, particularly during the forward and backward projection processes. These computations are pivotal in determining overlap extent and in defining the exact contribution of each phantom voxel to the associated detector area. The Shepp-Logan head phantom, comprising a $128 \times 128 \times 128$ volume, was employed to validate the method. Fig. 2 offers a schematic illustration of the distance-driven projection method used to calculate the contribution of each pixel to the corresponding detector area for a given projection angle, θ. As inferred from Fig. 2, this system matrix provides insights into the geometric aspects of the projection image acquisition process, encompassing the orientations and positions of the X-rays, detectors, and phantoms. The intricacy of these operations varies depending on the dimensions of the chosen detector and phantom, as depicted in Fig. 2. Consequently, a pivotal computation in tomosynthesis is the formation of the system matrix, a process that tends to be time-consuming.

2.3. Projector Acceleration

Considering the computational demands elaborated upon in section 2.2, tailored parallel optimization corresponding to the volume of data processed at each phase becomes imperative. Specifically, during the forward and backward projection phases, we aimed to parallelize the calculation of the contributions from each phantom voxel and detector pixel, ensuring accurate computation for every projection angle. The image reconstruction code utilizing projection operators has been adeptly implemented in Python 3.8 using the CUDA library. In this research, the GPU's maximum block size was optimized and determined to compute the overlay of specific phantom slices projected onto the 2D detector array. For computa-

Algorithm 1. Projection Operators

Forward and Backward Projection kernel (F, B)

W : system matrix

$P_{x,y,z}$: phantom position matrix, $N_{P_{x,y,z}}$ is number of phantom voxel size

$D_{u,v}$: detector position matrix, $N_{D_{u,v}}$ is number of detector pixel size

$S_{x,y,z}$: source position matrix, $N_{S_{x,y,z}}$ is number of source size

a. Host

i) Set the number of grids, blocks, and threads. ($N_{P_{x,y,z}}$, $N_{D_{u,v}}$)

ii) Global CUDA memory allocation of current phantom, detector position data set ($P_{x,y,z}$, $D_{u,v}$)

iii) Call a device kernel

b. Device

i) Assigning threads to each phantom voxel and detector pixel elements

for each angle calculation k = 0, 1, 2, ⋯, N_S **do**

  1) calculate the forward projection (F) and backward projection (B)

  2) save the system matrix

ii) CUDA synchronize.

Fig. 3. Pseudo programming of the proposed projection operators acceleration scheme.

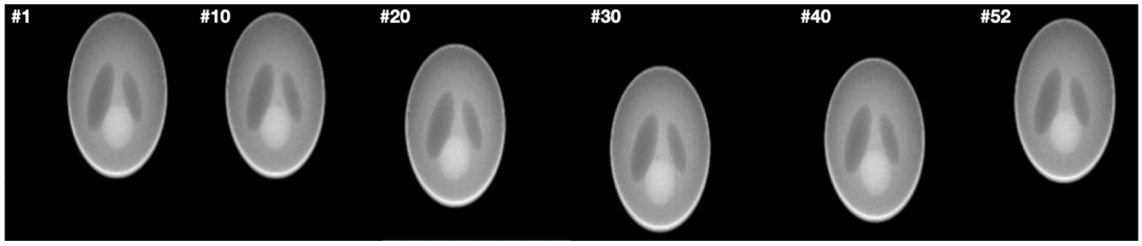

Fig. 4. Projection images utilizing the distance-driven technique in rectilinear geometry DTS system, and comprises a total of 52 distinct projection images.

tional efficiency, essential data including the positional and movement coordinates of X-rays, phantoms, and detectors is stored in GPU global memory, thereby mitigating potential overhead time associated with data transfer and kernel execution. To overcome memory contention issues arising from concurrent utilization of identical array elements during projection and back-projection, a barrier synchronization mechanism is employed post each block. Regarding computational hardware, our configuration primarily features an Intel Core i7-8700K, equipped with 6 cores and 12 threads, operating at a base frequency of 3.7 GHz and capable of turbo boosting up to 4.7 GHz. For GPU operations, we used the GeForce GTX 1080 Ti. This GPU, based on the Pascal architecture, incorporates 3584 CUDA cores, 28 streaming multiprocessors (SMs), and operates at a frequency of 1.58 GHz. Each GPU block comprises 65536 registers along with an added 48 KiB of shared memory. The expedited projection operator algorithm can be viewed in Fig. 3.

3. Results and Dicussion

In order to validate the feasibility of applying the rectilinear geometry DTS system to the LINAC system, 52 projection images of the Shepp-Logan phantom were initially obtained through simulation. Fig. 2 displays a selection of these projection images. These images clearly

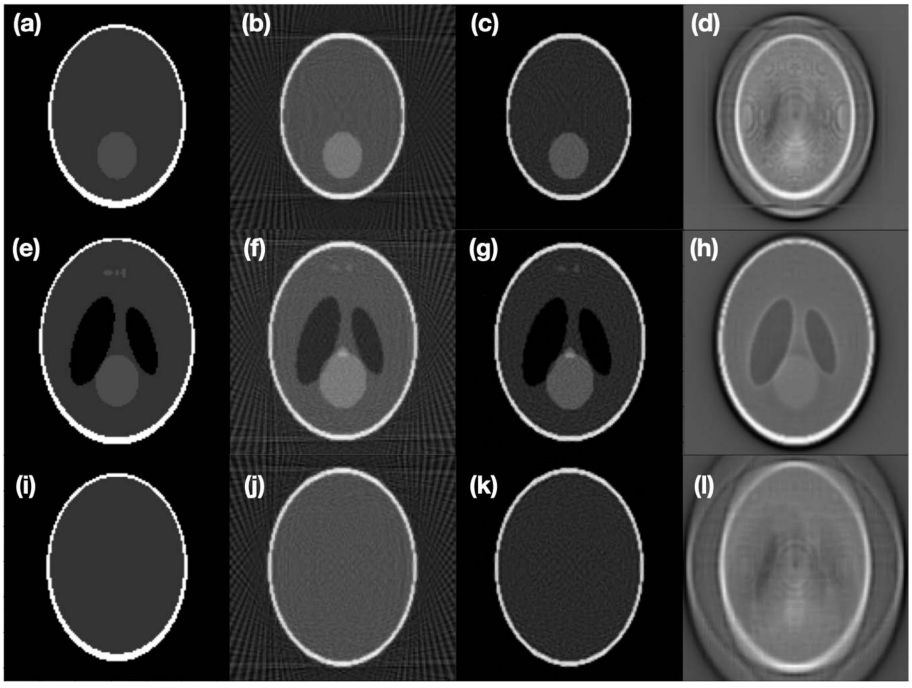

Fig. 5. Comparison of reference and reconstructed images. (a), (e), and (i) display the reference Shepp-Logan phantom images used for algorithm comparison. (b), (f), and (j) represent images reconstructed using the Feldkamp-Davis-Kress (FDK) method. (c), (g), and (k) represent images obtained through the iterative OSSART method with 100 iterations. Both the FDK and OSSART algorithms are based on 180 projection images in a 360 degree rotation for the reconstruction process. Lastly, (d), (h), and (l) represent images reconstructed via the filtered back projection (FBP) method in the rectilinear geometry digital tomosynthesis (DTS) system.

depict the geometric interactions between the 52 X-ray tubes, which are arranged in a rectangular configuration, and the stationary EPID at various positions. The projection images were acquired using the distance-driven technique, which had been accelerated with GPU-based CUDA programming. These images were then reconstructed employing the FBP algorithm. As shown in Fig. 5, the DTS reconstruction results were compared with images reconstructed with projection images obtained from CBCT geometry. For the CBCT image reconstruction, both the conventional FDK algorithm and the iterative reconstruction algorithm (OSSART), which are utilized in LINAC's on-board imaging (OBI) were employed [16]. The reconstructed images in the rectilinear geometry DTS system allow us to access the tomographic image that cannot be obtained from the two-dimensional projection image taken from the existing EPID. Additionally, it is possible to compare this tomographic image information with the 3D image reconstructed from the CBCT, which is widely used in current practices. Table 1 provides the forward- and backward-projection times in the FBP reconstruction algorithm with distance-driven technique which is accelerated using a GPU and those using only the CPU. A comparative analysis of the processing times between the GPU and CPU indicates that the GPU-accelerated image reconstruction achieved a performance approximately 30.09 % more faster than its CPU counterpart. While direct comparisons with other studies are challenging due to diverse experimental setups [17, 18], our results underscore the efficiency of using a single GeForce GTX 1080 Ti GPU for accelerating DTS image reconstruction time, which significantly reduced the processing time compared to CPU-based reconstructions. Our research also illuminates the promising application of the kV X-ray based rectilinear geometry DTS system for exact patient positioning in LINAC setups, a key component of EBRT, offering a distinctive angle on the use of GPU technology in medical imaging. The capacity for swift image reconstruction afforded by GPU acceleration could signal a pivotal progression in radiotherapy, promising to enhance both the precision of treatment and the overall patient care experience. The adoption of GPUs with capabilities that exceed those of the GeForce GTX 1080 Ti, along with the application of multi-GPU acceleration strategies [19], is projected to significantly reduce image reconstruction times. These technological advancements are poised to enable real-time image verification, thereby improving the accuracy of dose delivery in LINAC systems.

Table 1. Reconstruction time results for filtered back projection (FBP) with distance-driven method in the rectilinear geometry digital tomosynthesis (DTS) System.

	Hardware	
	CPU	GPU
Forward projection Time	785 sec	26.09 sec
Backward projection Time	812 sec	26.99 sec
Accelerated rate	-	~30.09

4. Conclusions

In this study, we validated the potential of the kV X-ray based rectilinear geometry DTS system for ensuring precise patient positioning, aiming for optimal treatment outcomes within the LINAC system, an EBRT setup. To facilitate real-time treatment, we accelerated the DTS image reconstruction process using GPU-based CUDA programming. The projection image essential for reconstruction was modeled and acquired through simulating the rectilinear geometry DTS system. Through this simulation, we obtained projection images, which we then reconstructed and compared using the FBP, FDK, and iterative (OSSART) algorithms The suitability for the LINAC system was ascertained by examining the 3D tomographic information present in the reconstructed images. Moreover, the feasibility of real-time positioning was confirmed by reducing the reconstruction time through GPU-based CUDA programming in the process of forward- and backward projection. Nonetheless, the rectilinear geometry DTS system demands an auxiliary cooling system to handle the heat produced during X-ray generation. Furthermore, DTS reconstructed images tend to exhibit compromised image quality on the upper and lower slices due to geometric dependencies. This often results in various artifacts like truncation and blurring, necessitating additional efforts to mitigate these artifacts. Based on these findings, we believe that it is feasible to position patients using reconstructed tomographic images in real-time using kV tomography images, even without the reliance on OBI.

Acknowledgment

This work was supported by the Dongseo University Research Fund of 2022 (DSU-20220018).

References

[1] D. A. Jaffray, Nat. Rev. Clin. Oncol. **9**, 688 (2012).
[2] L. A. Dawson and D. A. Jaffray, J. Clin. Oncol. **25**, 938 (2007).

[3] C. Western, D. Hristov, and J. Schlosser, Cureus. **7**, e280 (2015).
[4] J. Ng, F. Gregucci, R. T. Pennell, H. Nagar, E. B. Golden, J. P. S. Knisely, N. J. Sanfilippo, and S. C. Formenti, Front. Oncol. **13**, 1117874 (2023).
[5] J. J. W. Lagendijk, B. W. Raaymakers, A. J. E. Raaijmakers, J. Overweg, K. J. Brown, E. M. Kerkhof, R. W. v. d. Put, B. Hårdemark, M. v. Vulpen, and U. A. v. d. Heide, Radiother. Oncol. **86**, 25 (2008).
[6] D. Odero and D. Shimm, Biomed. Imaging. Interv. J. **5**, e25 (2009).
[7] D. A. Jaffray, J. H. Siewerdsen, J. W. Wong, and A. A. Martinez, Int. J. Radiat. Oncol. Biol. Phys. **53**, 1337 (2002).
[8] J. Prunaretty, P. Boisselier, N. Aillères, O. Riou, S. Simeon, L. Bedos, D. Azria, and P. Fenoglietto, Rep. Pract. Oncol. Radiother. **24**, 97 (2019).
[9] D. J. Godfrey, F. F. Yin, M. Oldham, S. Yoo, and C. Willett, Int. J. Radiat. Oncol. Biol. Phys. **65**, 8 (2006).
[10] S. Park, G. Kim, H. Cho, K. Kim, D. Lee, W. Kim, Y. Lim, and C. Seo, J. Instrum. **14**, C12004 (2019).
[11] J. C. Park, J. S. Kim, S. H. Park, M. J. Webster, S. Lee, W. Y. Song, and Y. Han, PLoS One. **9**, e115795 (2014).
[12] J. S. Maltz, F. Sprenger, J. Fuerst, A. Paidi, F. Fadler, and A. R. Bani-Hashemi, Med. Phys. **36**, 1624 (2009).
[13] J. C. Park, B. Song, J. S. Kim, S. H. Park, H. K. Kim, Z. Liu, T. S. Suh, and W. Y. Song, Med. Phys. **39**, 1207 (2012).
[14] M. A. Belzunce, C. A. Verrastro, E. Venialgo, and I. M. Cohen, Open J. Med. Imaging. **6**, 108 (2012).
[15] X. Jia, Y. Lou, R. Li, W. Y. Song, and S. B. Jiang, Med. Phys. **37**, 1757 (2010).
[16] A. Biguri, M. Dosanjh, S. Hancock, and M. Soleimani, Biomed. Phys. Eng. **2**, 055010 (2016).
[17] R. Cavicchioli, J. C. Hu, E. L. Piccolomini, E. Morotti, and L. Zanni, Sci. Rep. **10**, 1 (2020).
[18] D. Arefan, A. Talebpour, N. Ahmadinejhad, and A. K. Asl, J. Biomed. Phys. Eng. **5**, 83 (2015).
[19] X. Jia, P. Ziegenhein, and S. B. Jiang, Phys. Med. Biol. **59**, R151 (2014).